**ADVANCED
MATERIALS**

Communications

Near-Field Fluorescence Microscopy of Tris-8-hydroxyquinoline Aluminum Films**

By *Grace M. Credo* and *Steven K. Buratto**

We use near-field scanning optical microscopy (NSOM) to probe the local optical and morphological properties in drop-cast, spin-cast, and vacuum-deposited tris-8-hydroxy-quinoline aluminum (Alq_3) films with 10–100 nm resolution, the length scale of many interesting structural domains. We use concurrent shear force microscopy (an analog to atomic force microscopy, AFM) to correlate morphology (different regions) to intensity variations in our fluorescence images as well as variations in the localized fluorescence spectra. Our studies show that drop-cast films have the largest surface roughness and most spatial variation in film fluorescence while vacuum-deposited films have the smallest surface roughness and the least spatial variation in film fluorescence.

Thin films of the luminescent organic semiconductor Alq_3 have been widely studied due to their tremendous potential as the active layer in organic light-emitting devices (LEDs).[1–3] In contrast to the majority of conventional inorganic materials (III–V semiconductors) used in current generation LEDs, a large number of organic molecular semiconductors, such as Alq_3, have extremely high fluorescence efficiencies in the blue and green visible region. Large-scale production and purification of such materials is likely to be less costly than for current inorganic-based LEDs.[1] The use of a thin film of Alq_3 λ_{max} = 550 nm, green) as the emissive layer in a practical electroluminescent device constructed from layered organic materials was first demonstrated in 1987.[4] Despite the numerous spectroscopy techniques applied to Alq_3 films, the dependence of its nanoscale optical properties on film morphology, particularly on a submicrometer level, remains poorly understood.[5] Previous studies rely on far-field spectroscopy techniques that average over many morphological domains[6–8] or on topographical images taken without the benefits of concurrent optical probing.[9]

In this work, we apply NSOM to directly probe the nanoscale (10–100 nm) optical properties of Alq_3. NSOM allows

optical microscopy and spectroscopy with greater than 100 nm spatial resolution, a length scale where many of the optical and transport properties of Alq_3 are defined.[10] In NSOM, a sub-wavelength (10–200 nm) aperture is placed in close proximity to the surface of interest (near-field region ≈10 nm) and the interaction between laser light passing through the aperture and the sample is limited to the aperture diameter.[11] If the aperture is maintained in the near-field and scanned over a sample surface, an image can be reconstructed point by point with spatial resolution limited by the aperture diameter rather than by the wavelength of light (the diffraction limit, $\lambda/2$). The combination of the proximity of the tip to the sample and small tip aperture in NSOM has made it possible to achieve ultrahigh spatial resolution.

In our NSOM apparatus, depicted in Figure 1, a tapered fiber optic tip with laser light coupled to it is fixed while the sample, mounted film-side down on a piezo tube
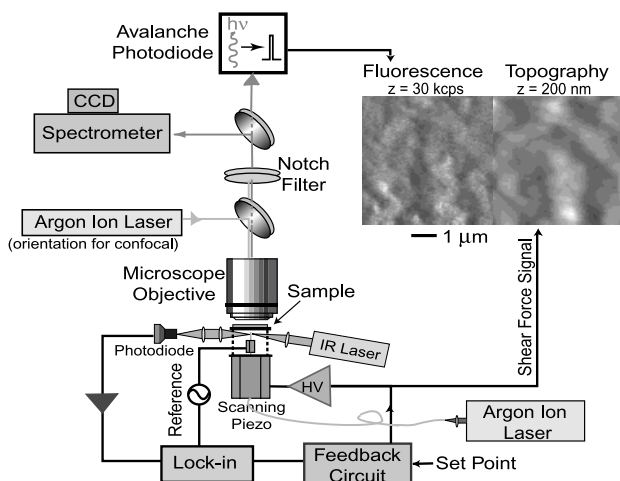

Fig. 1. Transmission NSOM apparatus block diagram. The photodiode detects IR laser light scattered by the dithered tip. This signal is used for optical shear force detection and is used in a feedback circuit to maintain the tip in the near-field of the sample. Transmitted fluorescence is collected in the far-field with a microscope objective. Using a beam splitter in the path of the collected fluorescence signal, emission intensity images and emission spectra can be acquired simultaneously.

(Stavely Sensors), is raster-scanned above it. The tip is used to excite the sample and the emission (fluorescence) that results in the sample is detected in the far-field using a 125× microscope objective (0.80 NA, Leitz). Using a beam splitter in the path of the transmitted signal we are able to collect spatially resolved fluorescence spectra simultaneously with integrated fluorescence imaging. Our tip apertures are typically 100 nm in diameter. The tip–sample distance, regulated by the standard optical shear force feedback mechanism, is approximately 10 nm.

[*] Prof. S. K. Buratto, G. M. Credo
Department of Chemistry
University of California at Santa Barbara
Santa Barbara, CA 93106-9510 (USA)

ADVANCED MATERIALS

We imaged the topography of the sample simultaneously with NSOM using shear force microscopy, an analog to attractive-mode atomic force microscopy (AFM). In shear force microscopy, the tapered optical fiber NSOM tip (diameter ~200 nm) is used to scan the surface of the sample.[12] This tip is attached to a small piezoelectric tube and dithered on resonance. The tip–sample distance is determined by monitoring the dither amplitude as the sample approaches the tip. The dither amplitude is measured by scattered laser light synchronously with the dither frequency. This provides the input for the feedback loop of our scanning electronics, shown in Figure 1, which is set to maintain a constant height above the sample surface (~10 nm).

Laser scanning confocal microscopy (LSCM) was also used to image the resulting films on glass with a spatial resolution of ~400 nm, as shown in Figures 2 and 3. The laser scanning confocal microscope has been described in detail elsewhere.[13] For LSCM, the same apparatus depicted in Figure 1 is used with the NSOM tip removed. For excitation, the 457.9 nm line of an Ar^+ laser (Spectra-Physics) was directed into the microscope and focused into a small spot using the objective used for NSOM. The resulting fluorescence is detected the same way as fluorescence NSOM, with the avalanche photodiode (APD) detector placed confocal with the excitation spot. An example of the intensity variations seen in local fluorescence spectra is shown in Figure 2.

Figure 2 presents a visual comparison of the resolution available with both NSOM and LSCM. Like the NSOM image, the confocal image shows irregularly shaped alternating regions of brightness and darkness. The notable difference is in feature resolution. The image taken with LSCM (Fig. 2A) has features that can be resolved to approximately 400 nm. Resolution much less than the diffraction limit (~100 nm) is obtained using NSOM (Fig. 2B), which shows features not visible in the corresponding LSCM image and nanoscale optical resolution not observed with previous techniques. As shown in Figure 2A, in the LSCM fluorescence image the fluorescence varies with depth of contrast of 50 %. In Figures 2B and 2C, the NSOM fluorescence throughout the film varies with depth of contrast of 71 % and 80 %, respectively. The fluorescence in these particular LCSM and NSOM images appears to be weakly correlated to surface topography, which has features that are 200 nm in height.

Additional fluorescence NSOM and shear force images of the same 10 μm thick Alq_3 film are shown in Figure 3. Samples of this film thickness were also characterized by scanning electron microscopy (SEM). In preparing this sample, silicon and silica substrates were positioned directly above the evaporating boat (~0.5 cm high). The Alq_3 was deposited very quickly (no deposition rate was established). For SEM, the silicon substrate was cleaved and the sample was imaged edge on. The SEM image (Fig. 3A) shows both large accumulations of Alq_3 and the void re-

A) LSCM Fluorescence

600 kcps

1 μm
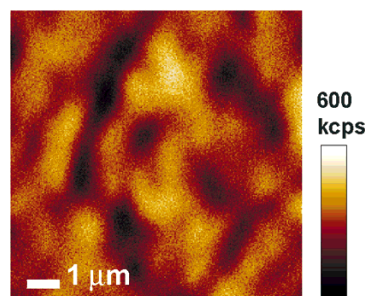
B) NSOM Fluorescence

35 kcps

1 μm
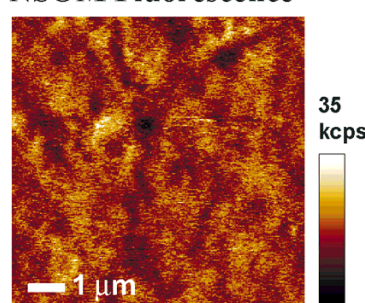
C) Shear Force Topography

200 nm

1 μm
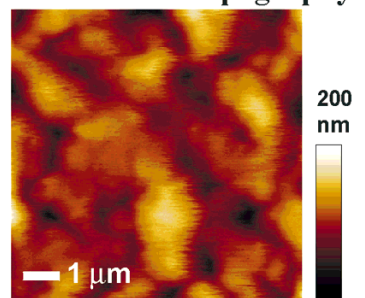
Fig. 2. Comparison of NSOM and LSCM. The image taken with LSCM (A) has features that can be resolved to approximately 400 nm. Depth of contrast in the LSCM image is 50 % and in the NSOM image 71 %. Resolution much less than the diffraction limit (~100 nm) is obtained using NSOM (B), which shows features not visible in the corresponding LSCM image and nanoscale resolution not observed with previous techniques. The shear force topography image, simultaneously obtained with (B), is shown in (C).

gions between them. The shear force topography image in Figure 3B correlates well with the features seen in SEM.

The shear force and NSOM images in Figure 2 were adjusted for maximum contrast. The shear force image (Fig. 3B) confirms the presence of large, hemispherical accumulations of Alq_3. The 100 nm tall features in the shear force topography image correlate to darker regions in the fluorescence image in Figure 3D. The brighter fluorescence regions correspond to the lower, void regions in the topography image. The anti-correlation of the NSOM fluorescence and shear force topography images is unexpected, but may be explained by considering the possibility that the Alq_3 morphology in the tallest regions contributes to decreased fluorescence yield, while the orientation of Alq_3 molecules in the crevices between the mounds promotes more efficient fluorescence. This type of variation in near-

 0935-9648/00/0302-0184 $ 17.50+.50/0
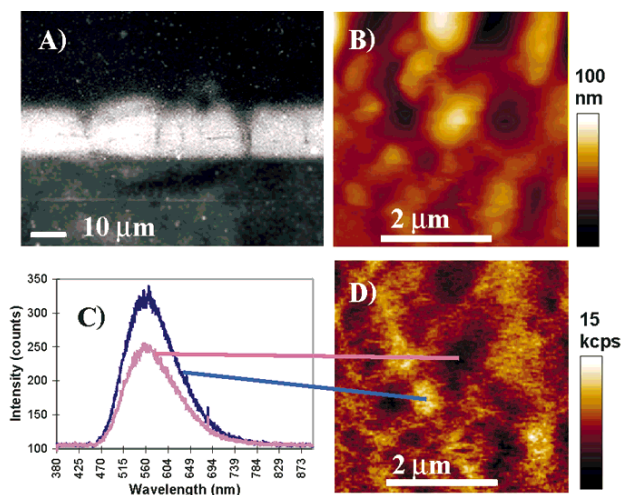
Fig. 3. Spatially resolved spectra of thick Alq_3 films. The 10 μm thick Alq_3 film was characterized by A) shear force topography, B) NSOM, and D) near-field optical spectroscopy (NFOS). The shear force and NSOM images have been adjusted for maximum contrast. Depth of contrast in the NSOM image is 80 %. The 100 nm tall features in the topography correlate to darker regions in the fluorescence image. The differences in local spectroscopy are illustrated by (C) which shows spectra characteristic of the darkest and brightest regions in the NSOM image.

field fluorescence intensity and its relationship to film morphology have been examined in thin films of PPV and its derivatives.[14]

With NSOM, it is possible to obtain spatially resolved spectra of different regions in Alq_3 films. The differences in local spectroscopy are illustrated by Figure 3C, which shows spectra characteristic of the darkest and brightest regions in the NSOM image. Although the spectra are similar in shape, indicating the presence of Alq_3 throughout the sample, the emission intensity in the spectrum from the darker region is approximately 1/3 less than that of the brighter region. This implies that the fluorescence NSOM image in Figure 3B indicates variations in the fluorescence quantum yield in the film.

In order to further understand the nanoscale morphology of Alq_3 and its influence on the material's optical properties, we compared fluorescence NSOM images of samples prepared by vacuum deposition, drop-casting, and spin-casting. As shown in Figure 4, there are notable differences among the three deposition methods of Alq_3 studied. In Figure 4A, both the fluorescence and topography are relatively uniform, indicative of a evenly deposited, homogeneous thin film, unlike the 10 μm Alq_3 film shown in Figures 2 and 3. For this film, the silica substrate was approximately 30 cm from the sample boat and the Alq_3 was deposited at a rate of 3 Å/s. Shear force topography scans of vacuum-deposited films had typical root mean square (rms) surface roughness of less than 1 nm.

In contrast, for both the spin-cast film (~20 nm thick) in Figure 4B and drop-cast film (~20 nm thick) in Figure 4C, the fluorescence and topography images are non-uniform when compared to the vacuum-deposited film. The spin-cast film in Figure 4B contains relatively large features
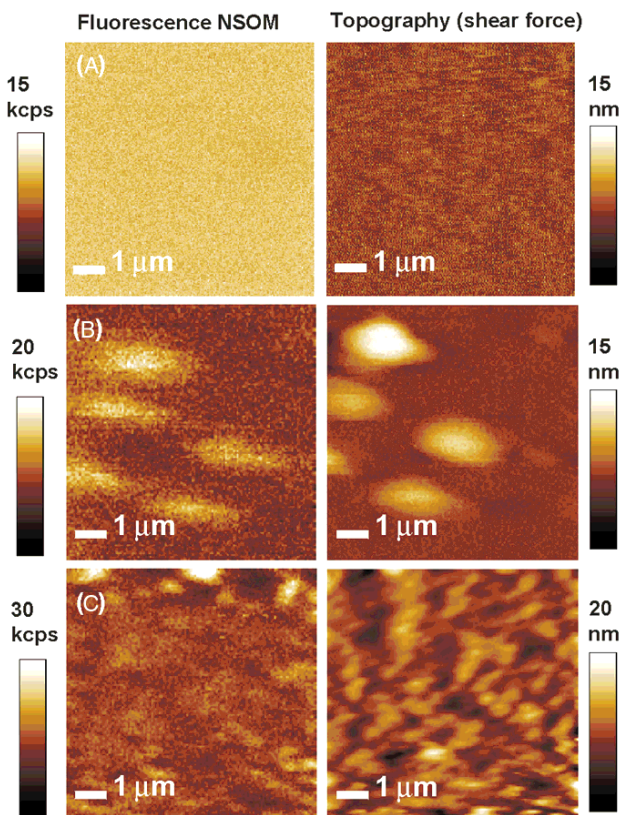

Fig. 4. Comparison of the effects of three deposition methods on Alq_3. The top two images (A) are the corresponding NSOM (left side) and shear force (right side) images of a 100 nm thick vacuum-deposited Alq_3 film on glass. The middle two images (B) are images of a 20 nm thick drop-cast film. The last two images (C) are of a 20 nm thick spin-cast film. The NSOM images in (B) and (C) have 56 % and 58 % depth of contrast, respectively.

when compared to both the vacuum-deposited film and the drop-cast film. Spin-cast films resulted in films of rms surface roughness equal to 2 nm. While the features are large, the height variation is not as frequent across the surface of the film. The spin-cast film image exhibits an increased fluorescence signal directly correlated to the aggregates visible in the topography images. In this case, increased film thickness, as seen in the brighter regions in the topography image, directly contributes to increased fluorescence efficiency.

In order to verify the relationship between film thickness and observed fluorescence intensity, we can compare the observed fluorescence signal to expected fluorescence signal. In general, thicker vacuum-deposited Alq_3 films exhibit increased absorption when compared to thinner vacuum-deposited films. The thicker films also exhibit increased emission when compared to thinner films. Using our topography image (Fig. 4B) to measure variations in film thickness, we can calculate the expected fluorescence emission increase for thicker regions of the film. For example, in the spin-cast film topography image, the difference between the highest features and the flat region of the film is 25 nm. With an overall film thickness of 20 nm, the largest feature, in the top left corner, corresponds to a 125 % difference in

ADVANCED MATERIALS

height. Assuming a linear relationship between thickness and absorption, as well as assuming a direct relationship between absorption and emission, the fluorescence signal, measured by NSOM, is expected to increase by the same percentage. The increase in fluorescence between the tallest feature and the background signal of 13 kcps is 13 kcps. Although this is not the total emission from the sample, since we have less than unity collection efficiency and we have placed a beam splitter in the path of the collected signal, as shown in Figure 1, we can compare the fluorescence percentage increase with the thickness percentage increase. Our observed fluorescence difference, as recorded in the NSOM image, is 100 %. This compares well to the percentage increase in topography.

In contrast to the spin-cast film, the drop-cast film in Figure 4C exhibits an increased fluorescence yield that is not correlated to topography. Although the shear force image indicates undulating surface topography throughout the film, regions of higher topography do not necessarily correspond to regions of increased fluorescence. Brighter regions in the shear force image are indicative of thicker regions in the irregular drop-cast film. For a sufficiently thin film, such as our 20 nm film, thicker regions would be expected to yield more fluorescence in a given area. In this case, the regions with the most fluorescence are not correlated with the highest regions in the topography image. As appears to be the case for the 10 μm Alq_3 film, variations in fluorescence may be due to local variations in the molecular packing of the Alq_3 molecules in film. In addition to the variation in fluorescence and topography, drop-cast films exhibited rms surface roughness of approximately 5 nm, the largest surface topography variation among the three deposition methods.

We have examined a variety of Alq_3 films (vacuum-deposited, drop-cast, and spin-cast) with confocal, near-field and shear force microscopy. NSOM allows direct probing of 10–100 nm features in Alq_3 films unseen in previous experiments. We found the vacuum-deposited Alq_3 film to be the most homogeneous film, both in terms of topography and fluorescence. In contrast, the drop-cast film had both the most varied surface topography and fluorescence, while the spin-cast film had large topographical features that directly correlated to increased local fluorescence efficiency.

Experimental

Glass coverslips (Fisher) were used as sample substrates. The slides were rinsed in acetone and flamed before use. Alq_3 powdered solids were used as received (Aldrich). Several samples were vacuum-deposited purified Alq_3 (Thompson Group, USC) thin films. The solids were placed in a baffled tungsten evaporating boat (R. D. Mathis) and sublimed at low pressures (~10^{-6} torr). The samples were stored in air. For spin-cast films, a stock solution (3.0×10^{-4} M) of Alq_3 in acetone was made. The glass substrate was fixed to the stage of a homemade spin coater as 10 μL aliquots of the solution were dropped onto the center of spinning glass (~3500 rpm). In addition, several Alq_3 films were made by allowing a drop of the stock solution to dry on a glass slide (drop casting). For vacuum-deposited films, sample

thickness was determined by a quartz crystal thickness monitor. Spin-cast and drop-cast film thicknesses were determined by profilometer (Sloan Dektak II).

[1] J. R. Sheats, H. Antoniadis, M. Hueschen, W. Leonard, J. Miller, R. Moon, D. Roitman, A. Stocking, *Science* **1996**, *273*, 884.
[2] H. Aziz, Z. D. Popovic, N.-X. Hu, A.-M. Hor, G. Xu, *Science* **1999**, *283*, 1900.
[3] A. Curioni, M. Boero, W. Andreoni, *Chem. Phys. Lett.* **1998**, *294*, 263.
[4] C. W. Tang, S. A. VanSlyke, *Appl. Phys. Lett.* **1987**, *51*, 913.
[5] G. E. Jabbour, S. E. S. Y. Kawabe, J. F. Wang, M. M. Morrell, B. Kippelen, N. Peyghambarian, *Appl. Phys. Lett.* **1997**, *71*, 1762.
[6] M. Fujihira, L.-M. Do, A. Koike, E.-M. Han, *Appl. Phys. Lett.* **1996**, *68*, 1787.
[7] F. Papadimitrakopoulos, X. M. Zhang, D. L. Thomsen, K. A. Higginson, *Chem. Mater.* **1996**, *8*, 1363.
[8] A. D. Walser, I. Sokolik, R. Priestley, R. Dorsinville, *Synth. Met.* **1997**, *84*, 877.
[9] K. Yase, S.-S. Sumimoto, H. Matsuda, M. Kato, *Mol. Cryst. Liq. Cryst.* **1995**, *267*, 151.
[10] P. E. Burrows, Z. Shen, V. Bulovic, D. M. McCarty, S. R. Forrest, J. A. Cronin, M. E. Thompson, *J. Appl. Phys.* **1996**, *79*, 7991.
[11] E. Betzig, J. K. Trautman, T. D. Harris, J. S. Weiner, R. L. Kostelak, *Science* **1991**, *251*, 1468.
[12] E. Betzig, P. L. Finn, J. S. Weiner, *Appl. Phys. Lett.* **1992**, *60*, 2484.
[13] K. D. Weston, S. K. Buratto, *J. Phys. Chem. A* **1998**, *102*, 3635.
[14] J. A. DeAro, K. D. Weston, S. K. Buratto, U. Lemmer, *Chem. Phys. Lett.* **1997**, *277*, 532.

Two-Dimensional Crosslinked Nanoparticle Networks**

By *Shaowei Chen*

Fabrication of ordered arrays of nanoelectrodes and nanoclusters have recently attracted extensive research interest, due to the fundamental and technological significance associated with these nanoscale architectures.[1–8] One of their most striking characteristics is the so-called quantum effect that arises from the nanosized dimensions of the materials, demonstrated by various unique properties that are vastly different from those of single molecules or the bulk phase.[9–11] As their diverse application potentials are largely limited to the availability of methodologies for the fabrication of organized assemblies in a controllable fashion, a great deal of research effort has been focused on the development of different approaches.

Among the materials studied, monolayer-protected nanoclusters (MPCs)[12,13] emerged as a distinct member of the rapidly expanding family of advanced nanomaterials, which exhibit great stability in both solution and dry forms, in contrast to conventional colloidal particles. The development of new methods for the fabrication of their ordered ensembles might help pave the way towards their applications as the structural basis for electronic nanocircuits/

[*] Prof. S. Chen
Department of Chemistry and Biochemistry
Southern Illinois University
Carbondale, IL 62901-4409 (USA)